

M. SZOTA*[#]**EFFECT OF SMALL ADDITION OF COBALT ON MAGNETIC PROPERTIES AND INTERNAL STRESSES SOURCES IN THE FORM OF FREE VOLUMES AND PSEUDO-DISLOCATION DIPOLES IN $\text{Fe}_{78}\text{Co}_x\text{Si}_{11-x}\text{B}_{11}$ ($x = 0$ OR 2) ALLOYS****WPLYW NIEZNACZNEGO DODATKU KOBALTU NA WŁAŚCIWOŚCI MAGNETYCZNE ORAZ ŹRÓDŁA NAPRĘŻEŃ WEWNĘTRZNYCH W POSTACI WOLNYCH OBJĘTOŚCI ORAZ PSEUDODYSLOKACYJNYCH DIPOLI W STOPACH $\text{Fe}_{78}\text{Co}_x\text{Si}_{11-x}\text{B}_{11}$ ($x = 0$ LUB 2)**

Amorphous materials in the form of tapes, despite being discovered more than half a century ago, are still the object of interest for materials engineers and electro-technical industry. They possess a great application potential, and are constantly studied for new variations. Due to the different structure from the commonly manufactured textured FeSi sheets, FeCoB based amorphous alloys demonstrate very good, so called soft magnetic properties. This paper presents the results of studying the structure and magnetic properties of tapes of $\text{Fe}_{78}\text{Co}_x\text{Si}_{11-x}\text{B}_{11}$ ($x = 0$ or 2) alloys of amorphous structure. In addition, the effect of Co alloy addition on the type of structural defects in the area of ferromagnetic saturation approach was examined. It was found that a small addition of Co affects the increase of saturation magnetization value, as well as the distribution of magnetization vectors within the stresses sources in form of structure defects.

Keywords: amorphous alloys, soft magnetic materials, exchange interactions, Holstein-Primakoff paraproces

Materiały amorficzne w postaci taśm pomimo, że zostały odkryte już ponad pół wieku temu cały czas są obiektem zainteresowania inżynierów materiałowych i przemysłu elektrotechnicznego. Posiadają one ogromny potencjał aplikacyjny i stale poszukiwane są nowe ich odmiany. Ze względu na odmienną strukturę, niż w powszechnie produkowanych teksturowanych blachach FeSi, stopy amorficzne na bazie FeCoB posiadają bardzo dobre tzw. właściwości magnetyczne miękkie. W pracy przedstawiono wyniki badań struktury oraz właściwości magnetycznych dla taśm stopów $\text{Fe}_{78}\text{Co}_x\text{Si}_{11-x}\text{B}_{11}$ ($x = 0$ lub 2) o strukturze amorficznej. Ponadto, zbadano wpływ dodatku stopowego Co na rodzaj defektów strukturalnych w obszarze podejścia do ferromagnetycznego nasycenia. Stwierdzono, że niewielki dodatek Co wpływa na podniesienie wartości magnetyzacji nasycenia oraz rozkład wektorów magnetyzacji w obrębie źródeł naprężeń w postaci defektów struktury.

1. Introduction

The power industry based on electricity is a branch that determines the further development of our civilization. Therefore, materials engineers constantly seek for new types of alloys demonstrating unique magnetic properties [1]. In the electro-technical industry the greatest energy losses occur when transmitting electrical current over the network and during the transformers operation. The material commonly used for the production of cables is copper, and of transformers – FeSi sheets, respectively. Both copper cables and FeSi sheets can be replaced with one of the most modern metal functional materials, namely amorphous materials [2, 3]. In case of those alloys based on Fe combined with various alloy additions, it is possible to obtain a hysteresis loop, which area, given high magnetic induction, tends to zero [4]. It means that such material will easily undergo magnetization reversal. In addition amorphous alloys, when maintaining

proper chemical composition, may demonstrate almost zero magnetostriction, which makes them environmentally friendly. To produce such an alloy it is necessary to obtain appropriately high rate of solidification process, which can be done by omitting the crystallization process [5]. The most popular and known methods allowing the production of amorphous alloys include the technique of continuous unidirectional casting the stream of molten alloy on the copper spinning cylinder (melt-spinning). The cooling rate that can be achieved with this method is even 10^6K/s [6]. This technique is usually used to produce samples in the form of tapes of thickness not exceeding $100\mu\text{m}$ [7]. In general, the description of the structure defects in amorphous materials is difficult, as they do not contain symmetrical and repetitive areas of atoms systems that form the structure pattern.

According to the research published in [8, 9], one can indirectly observe sources of internal stresses in the form of structural defects in the volume of amorphous tapes. In

* CZESTOCHOWA UNIVERSITY OF TECHNOLOGY, FACULTY OF PRODUCTION ENGINEERING AND MATERIALS TECHNOLOGY, INSTITUTE OF MATERIALS ENGINEERING, 19 ARMII KRAJOWEJ AV., 42-200 CZĘSTOCHOWA, POLAND

[#] Corresponding author: mszota@wp.pl

amorphous alloys there occur free volumes (Fig. 1) as an equivalent of vacancies, and pseudo-dislocation dipoles (Fig. 1) as an equivalent of linear defects [10].

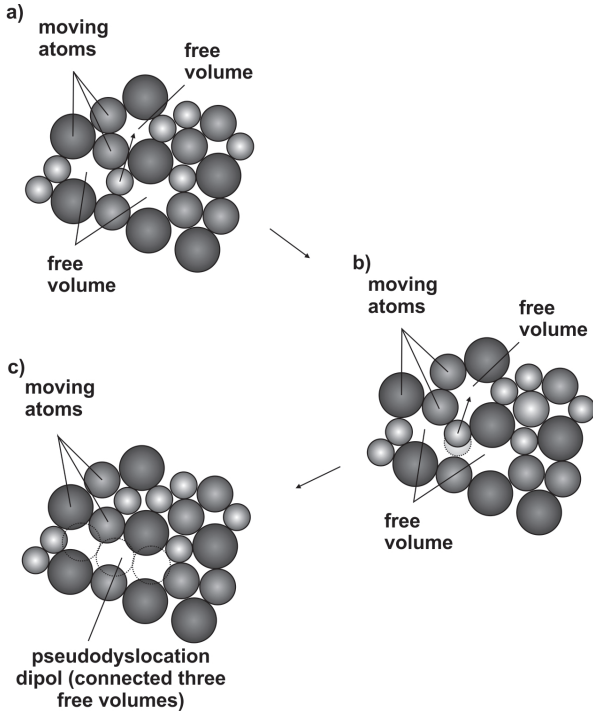


Fig. 1. Model of free volume and process of formation of pseudo-dislocation dipole as a result of free volumes conglomeration [10]

Fig. 1 presents schematically a free volume (a) and the process of formation of pseudo-dislocation dipole (b and c). The presence of structural defects, and more precisely their number and type have decisive significance in regard of the magnetization process of amorphous materials in strong magnetic fields [11]. In higher magnetic fields above the effective anisotropy field (K_{eff}), the magnetization can be described with the equation:

$$\Delta M = \Delta M_{\text{wev}} + \Delta M_{\text{para}} + \Delta M_{\text{def}} \quad (1)$$

where: (ΔM_{para}) – is related to the suppression of thermally induced spin waves by an external magnetic field; (ΔM_{wev}) – corresponds to internal fluctuations such as anisotropy or density change; (ΔM_{def}) – results from the existence of structural defects.

The factor ΔM_{wev} present in the equation has a minimal contribution in the process of magnetization, hence it shall be ignored in further considerations [12]:

$$\mu_0 M(H) = \mu_0 M_s \left[1 - \frac{a_{1/2}}{(\mu_0 H)^{1/2}} - \frac{a_1}{(\mu_0 H)^1} - \frac{a_2}{(\mu_0 H)^2} \right] + b(\mu_0 H)^{1/2} \quad (2)$$

where: M_s – spontaneous magnetization; μ_0 – magnetic permeability of vacuum; H – magnetic field strength; $a_{1/2}$, a_1 , a_2 – directional coefficients of linear fit, related to the structural defects; b – directional coefficient of linear fit corresponding to the suppression of thermally induced spin waves by an external magnetic field of high strength.

The factors present in the equation 2, related to the expression ΔM_{def} are described with the dependencies 3, 4 and 5 [13, 14].

$$\frac{a_{1/2}}{(\mu_0 H)^{1/2}} = \mu_0 \frac{3}{20 A_{\text{ex}}} \left(\frac{1+r}{1-r} \right)^2 G^2 \lambda_s^2 (\Delta V)^2 N \left(\frac{2 A_{\text{ex}}}{\mu_0 M_s} \right)^{1/2} \frac{1}{(\mu_0 H)^{1/2}} \quad (3)$$

$$\frac{a_1}{\mu_0 H} = 1,1 \mu_0 \frac{G^2 \lambda_s^2}{(1-\nu)^2} \frac{N b_{\text{eff}}}{M_s A_{\text{ex}}} D_{\text{dip}}^2 \frac{1}{\mu_0 H} \quad (4)$$

$$\frac{a_2}{\mu_0 H^2} = 0,456 \mu_0 \frac{G^2 \lambda_s^2}{(1-\nu)^2} \frac{N b_{\text{eff}}}{M_s^2} D_{\text{dip}}^2 \frac{1}{(\mu_0 H)^2} \quad (5)$$

where: ΔV – represents the change in volume caused by the existence of point defects determined by the volume density N ; A_{ex} – exchange constant; G – shear modulus; r – Poisson ratio; λ_s – magnetostriction constant.

Equations 3 and 4 include the expression A_{ex} which is called the exchange constant [15]:

$$A_{\text{ex}} = \frac{M_s D_{\text{spf}}}{2 g \mu_B} \quad (6)$$

Another expression ΔM_{para} present in equation (1) is described by the dependency 6.

$$b = 3,54 g \mu_0 \mu_B \left(\frac{1}{4\pi D_{\text{spf}}} \right)^{3/2} kT (g \mu_B)^{1/2} \quad (7)$$

where: k – Boltzmann constant; μ_B – Bohr magneton; g – gyromagnetic ratio, spin wave stiffness parameter.

Using dependencies 3-5 it is possible to determine the type and density of structural defects in amorphous materials.

The paper presents the results of structure and magnetic properties study for two amorphous alloys $\text{Fe}_{78}\text{Si}_{11}\text{B}_{11}$ i $\text{Fe}_{78}\text{Co}_2\text{Si}_9\text{B}_{11}$ in the form of tapes. In addition the analysis of initial magnetization curves was conducted and type and density of structure defects were determined.

2. Research methodology

The research samples were produced using components of high purity (<99,98). Crystalline ingots of alloys were prepared using electric arc furnace in protective gas atmosphere (Ar). Then they were crushed into smaller pieces that were melted in the induction furnace. The liquid metal was cast on copper wheel rotating with the linear speed of 35m/s. The resulting samples had a thickness of 35 μm .

The structure of tapes was examined using the BRUKER X-ray machine, model ADVANCE D8. The samples were cut into small petals and scanned at an angle of 2θ from 30° up to 120° with an exposure time of 7s. The structure of alloys was also studied using Mössbauer spectroscopy on POLON equipment. Those measurements employed Mössbauer source $\text{Co}57$. Using NORMOS software for Mössbauer spectra analysis allowed to obtain distributions of hyperfine fields induction at the ^{57}Fe nuclei. The initial magnetization

curves were measured in the range up to 2T, using vibrating magnetometer manufactured by LakeShore.

3. Research results

Fig. 2 presents images of X-ray diffraction obtained for research samples of alloys $\text{Fe}_{78}\text{Si}_{11}\text{B}_{11}$ and $\text{Fe}_{78}\text{Co}_2\text{Si}_9\text{B}_{11}$.

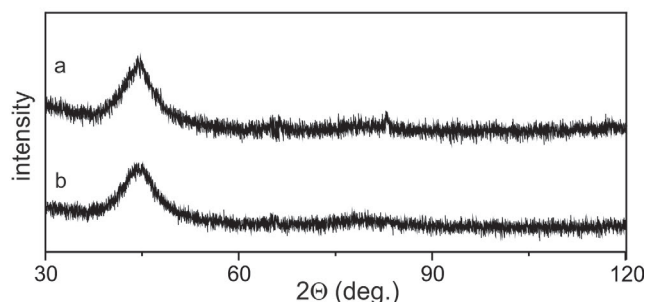


Fig. 2. X-ray diffractograms for samples: a) $\text{Fe}_{78}\text{Si}_{11}\text{B}_{11}$ i b) $\text{Fe}_{78}\text{Co}_2\text{Si}_9\text{B}_{11}$

X-ray diffractograms shown in Fig. 2 have a shape typical for amorphous materials [16, 17]. They consist only of the background of low intensity and wide single maximum appearing in the angle range from 40° to 55° .

The structure of alloys was also studied using Mössbauer spectroscopy. Obtained transmission Mössbauer spectra are presented in Fig. 3.

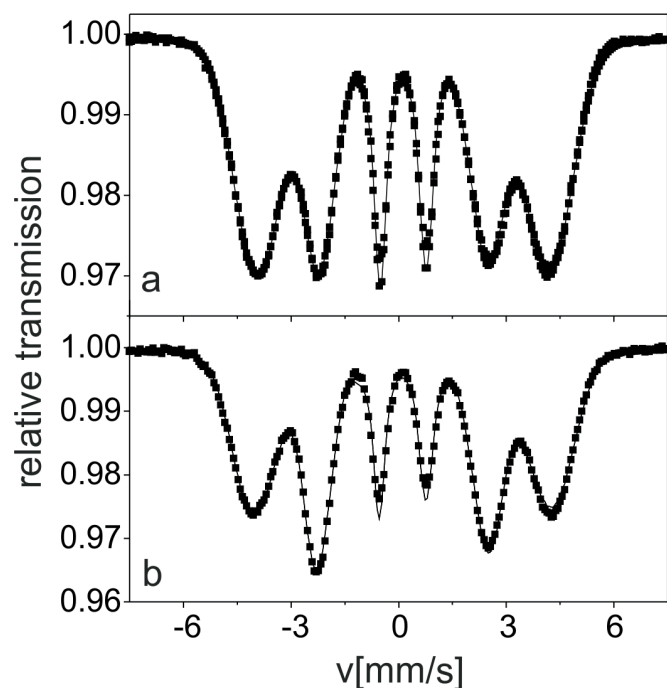


Fig. 3. Mössbauer spectra for the alloys: a) $\text{Fe}_{78}\text{Si}_{11}\text{B}_{11}$ i b) $\text{Fe}_{78}\text{Co}_2\text{Si}_9\text{B}_{11}$

The Mössbauer spectra presented in Fig. 3 consist of six wide overlapping lines, which is characteristic for ferromagnetic materials with amorphous structure [18]. Based on the analysis of those spectra using NORMOS software a distribution of hyperfine fields induction at the ^{57}Fe nuclei was developed (Fig. 4).

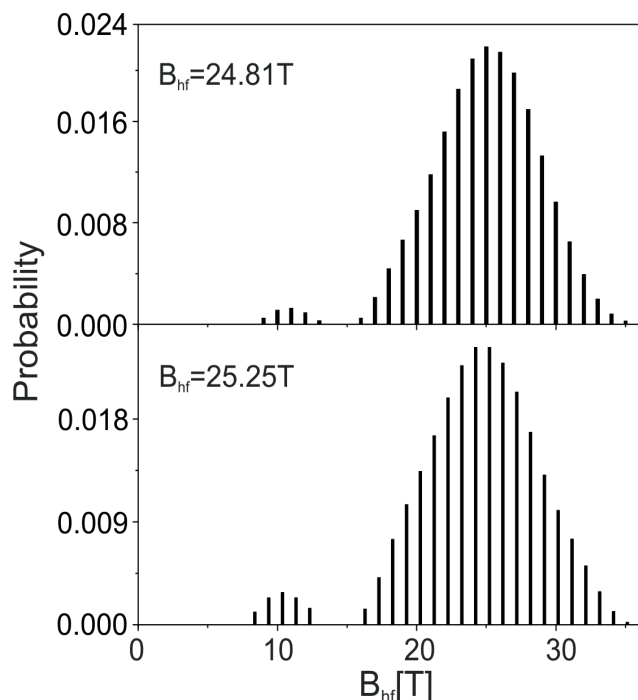


Fig. 4. Distributions of hyperfine fields induction for research samples: a) $\text{Fe}_{78}\text{Si}_{11}\text{B}_{11}$ i b) $\text{Fe}_{78}\text{Co}_2\text{Si}_9\text{B}_{11}$

Distributions of hyperfine fields induction consist of two clearly separated humps. The low field component has a maximum value of medium hyperfine field in the field of induction of 10-11 T. The average value of the distribution of hyperfine fields induction for low field component depends on the Co content in the alloy.

It is assumed that this component is related to Fe atoms and small distances between them, as well as to the presence of atoms of other elements forming the alloy [19]. The existence of Si or B in the first coordination layer of Fe for crystalline structure of BBC should significantly decrease the hyperfine field. In addition, if the volume of the alloy includes the areas rich in Co (over 74%) there can occur the formation of HCP crystalline structure. It is due to the presence of areas of cubic symmetry. Such systems includes twelve closest neighbours to the central atom. The studied alloys did not exhibited the presence of crystalline cells described above, but it can be assumed that the positions of atoms are similar to those positions without the repeatability and angle relations. It is known that Mössbauer research allow to obtain information about the closest environment of Fe atoms [20, 21], thus the changes in spatial distribution of components induced by the redistribution of moments of magnetic pairs (Fe-Fe, Fe-Co, Co-Co) and of pairs surrounding them (Fe-B, Fe-Si) depend exclusively on the speed of atoms diffusion during the solidification.

The second hump reaches its maximum value of medium hyperfine field in the field of the induction of about 25 T. Due to the presence of low field and high field components it can be stated, that the volume of studied alloys contains areas of different concentration of iron. The value of average hyperfine field induction B_{hf} for FeSiB sample is 24,81 T, while for FeCoSiB sample the value of B_{hf} equals 25,25 T. Greater value of B_{hf} represents the higher density of atoms distribution in the alloy with the addition of cobalt.

Fig. 5 illustrates the initial magnetization curves measured for studied alloys.

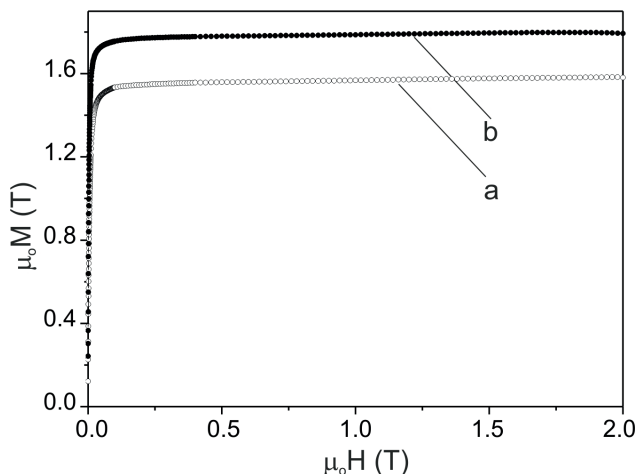


Fig. 5. Magnetization curves for amorphous alloys in the form of tapes: a) $\text{Fe}_{78}\text{Si}_{11}\text{B}_{11}$ i b) $\text{Fe}_{78}\text{Co}_2\text{Si}_9\text{B}_{11}$

Studied alloys demonstrate quite a high value of saturation magnetization, which for both alloys equals about 1.6T. Introducing into the alloy just 2% of Co atoms replacing Si causes the increase in saturation magnetization by as much as 0.4T. The observed increase in saturation magnetization is related to the increase of exchange interactions strength, which probably is the result of the formation of structures similar to FeCo crystalline systems.

Based on the study of magnetization in strong magnetic fields, the type and density of structure defects were determined using Kronmuller theories [12]. Fig. 6 presents high field magnetization curve for FeSiB sample.

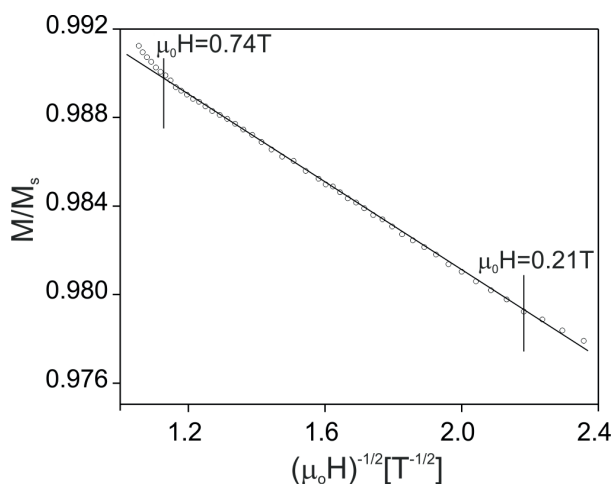


Fig. 6. The linear relationship of reduced magnetization $M/M_S(\mu_0H)^{-1/2}$ for FeSiB alloy

The linear relationship of reduced magnetization in the function of magnetic field indicates that the process of magnetization in the range of magnetic fields from 0.21 T to 0.74T is related to rotation of magnetization vector in the vicinity of point defects. In case of the sample including cobalt addition the decisive effect on magnetization in strong fields is exerted by so called pseudo-dislocation dipoles, for which 3 relation is met (Fig. 7).

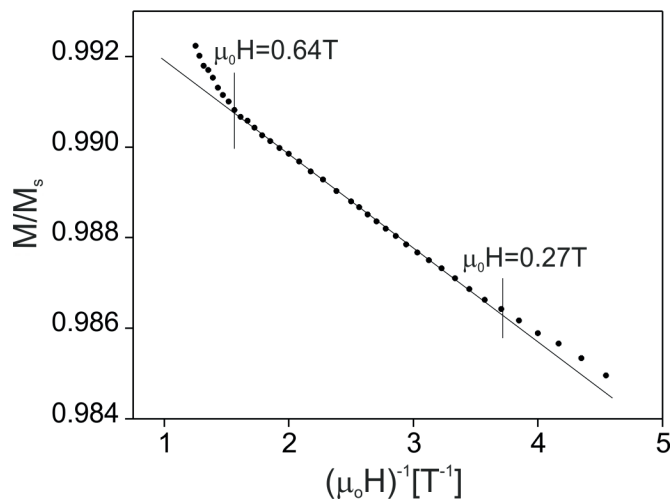


Fig. 7. The linear relationship of reduced magnetization $M/M_S(\mu_0H)^{-1}$ for FeCoSiB alloy

In higher magnetic fields in case of both samples the Holstein-Primakoff paraprocess was observed (Fig. 8) [22].

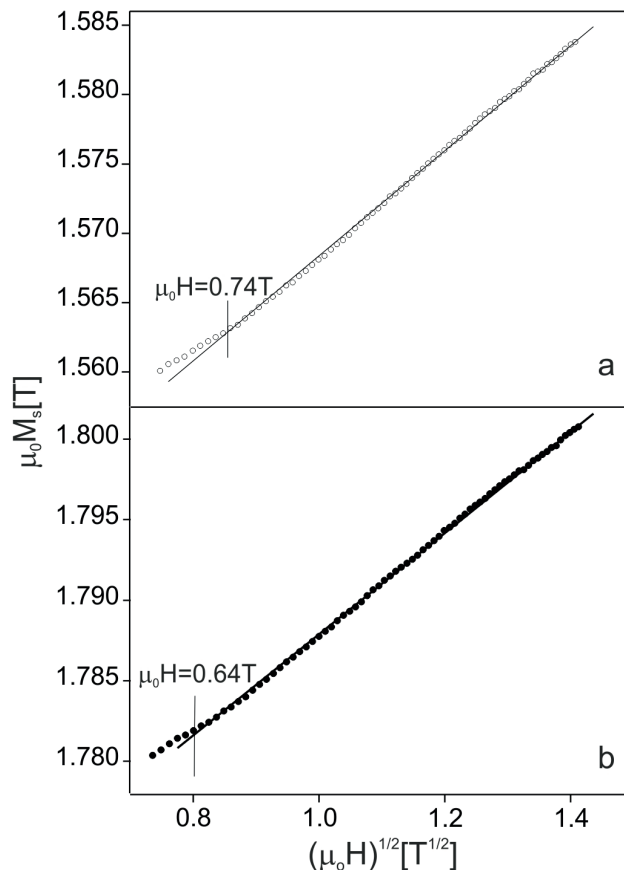


Fig. 8. The linear relationship of reduced magnetization $M/M_S(\mu_0H)^{1/2}$ for alloys: a) $\text{Fe}_{78}\text{Si}_{11}\text{B}_{11}$ i b) $\text{Fe}_{78}\text{Co}_2\text{Si}_9\text{B}_{11}$

In magnetic fields above 0.74 T and 0.64 T, for FeSiB and FeCoSiB samples, respectively, the linear relationship $M/M_S(\mu_0H)^{1/2}$ is observed. In this case a small increase of magnetization is caused by the suppression of thermally induced spin waves by a magnetic field (the Holstein-Primakoff paraprocess) [22, 23].

Parameters collected on the basis of magnetization curves analysis are presented in Table 2.

TABLE 1

Parameters collected from magnetization curves analysis: M_S – saturation magnetization; coefficients: $a_{1/2}$, a_1 , related to the presence of structural defects; „b” parameter related to the Holstein-Primakoff paraprocess; D_{spf} – spin wave stiffness parameter

| Parameters Samples | M_S [T] | $a_{1/2}$ [T ^{1/2}] | a_1 [T ⁻¹] | b [T ^{1/2}] | D_{spf} [10 ⁻² eVnm ²] |
|-----------------------|--------------|----------------------------------|-----------------------------|--------------------------|--|
| FeSiB | 1.58 | 0.0156 | | 0.039 | 58 |
| FeCoSiB | 1.63 | | 0.0021 | 0.033 | 64 |

Using the equation [24]:

$$D_{spf} = 1/3 S J_{ex}(a) a^2 z_m \quad (8)$$

where: S – the spin value in the distance from the central atom; J_{ex} – the local exchange integral; a – the distance to the nearest-neighbour atoms; z_m – the number of nearest-neighbour magnetic atoms, the parameter D_{spf} was determined. This parameter is connected with the changes in the nearest neighbourhood of the iron atoms. Higher value of this parameter for FeCoSiB alloy sample indicates the greater number of magnetic atoms and smaller distances between them, and thus the higher density of distribution of magnetic atoms in the alloy with the addition of cobalt [25]. Such result is consistent with the results of Mössbauer research (higher B_{hf} for FeCoSiB sample).

4. Conclusions

Using the melt-spinning method FeSiB and FeCoSiB alloys samples were produced in the form of tapes of amorphous structure. The structure of such materials is usually characterized as a function of atom pairs distribution. Physical and chemical characteristics of amorphous alloys, as in the case of other metallic materials are determined by the analysis of their microstructure. In amorphous materials, fluctuations of composition and density occur, which leads to the formation of structural and chemical order of intermediate range. During the solidification there occur some internal stresses of intermediate range in the volume of amorphous alloys. Those stresses are elastic.

For FeSiB alloy sample in the range of magnetic field from 0.21 T to 0.74 T a linear relationship of magnetization was observed, consistent with the 3 law of ferromagnetic saturation approach, while for the second of studied alloys the linear relationship was related to the 4 law of ferromagnetic saturation approach [9, 12, 14, 26]. It means that the introduction of Co into the alloy, replacing Si resulted in the change of diffusion processes in the phase of solidification. FeSiB sample demonstrated only the effect of point defects on the magnetization process, while after introducing Co they started to diffuse towards the surface of the sample and conglomerate into larger clusters, forming two-dimensional pseudo-dislocation dipoles.

In case of the sample with the addition of Co a greater so called topological order was observed, which means that the volume of this alloy incorporates more similar to each

other configurations of atoms in relation to the central atom, namely Fe. The density of magnetic atoms distribution can be determined indirectly using the analysis of results of magnetic polarization study as a function of magnetic induction in high magnetic fields in the range of the Holstein-Primakoff paraprocess. The value of the spin wave stiffness parameter (D_{spf}) for the sample of the alloy with the addition of Co is higher, which, according to [24], means that distances between the closest magnetic neighbours are smaller than in case of the other alloy. Most likely it is related to the formation of the chemical order of intermediate range.

If the sample is produced applying the longer solidification time, atoms have more opportunities to distribute across the volume of the alloy. The diffusion of atoms occurs at larger distances and stresses are partially offset. It is commonly known that proper heat treatment of ferromagnetic alloys enhances their properties [27].

In summary, only small amount of Co in magnetic alloys can significantly affect the redistribution of magnetic components in the volume of solidified material and increase the saturation magnetization.

REFERENCES

- [1] K. Błoch, M. Nabiałek, J. Gondro, *Mater. Tehnol.* **49**, 4, 553-556 (2015).
- [1] M. Nabiałek, P. Pietrusiewicz, M. Szota, M. Dośpiał, J. Jędryka, K. Szota, S. Lesz, *Arch. Metall. Mater.* **57**, 1, 223–227 (2012).
- [1] J. Gondro, K. Błoch, M. Nabiałek, K. Waltters, M. Szota, *Arch. Metall. Mater.* **60**, 1071-1074 (2015).
- [1] P. Pietrusiewicz, M. Nabiałek, M. Szota, K. Perduta, *Arch. Metall. Mater.* **57**, 1, 265–270 (2012).
- [1] M. Dospial, J. Olszewski, M. Nabialek, P. Pietrusiewicz, T. Kaczmarzyk, *Nukleonika* **60**, 15-18 (2015)
- [1] B. Karpe, B. Kosec, M. Bizjak, *JAMME* **51/2**, 59-66 (2012).
- [1] M. Nabiałek, P. Pietrusiewicz, K. Błoch, *J. All. Compd.* **628**, 424–428 (2015).
- [1] M. Nabiałek, P. Pietrusiewicz, M. Dośpiał, M. Szota, J. Gondro, K. Gruszka, A. Dobrzańska-Danikiewicz, S. Walters, A. Bukowska, *J. All. Compd.* **615**, S56–S60 (2014).
- [1] H. Kronmüller, *Micromagnetism and microstructure of amorphous alloys*, *J. Appl. Phys.* **52**, 1859 (1981).
- [1] M. Nabialek, P. Pietrusiewicz, M. Dospial, M. Szota, K. Błoch, K. Gruszka, K. Ożga, S. Garus, *J. All. Compd.* **615**, S51–S55 (2014)
- [1] M. Nabialek, M. Dospial, M. Szota, P. Pietrusiewicz, *Mat. Sci. Forum* **654-656**, 1074-1077 (2010).
- [1] H. Kronmüller, M. Fähnle, *Micromagnetism and the microstructure of ferromagnetic solids*, *Cambridge University Press* **2003**
- [2] H. Kronmüller, *J. Appl. Phys.* **52**, (3), 1859–1864 (1981).
- [3] O. Kohmoto, *J. Appl. Phys.* **53** (11) 7486–7490 (1982).
- [4] H. Kronmüller, *General Micromagnetic Theory*, *Handbook of Magnetism and Advanced Magnetic Materials*, John Wiley & Sons, (2) (2007)
- [5] M. Dospial, J. Olszewski, M. Nabialek, P. Pietrusiewicz, T. Kaczmarzyk, *Nukleonika* **60**, 15-18 (2015).
- [6] K. Gruszka, M. Nabiałek, K. Błoch S. Walters, *Int J Mater Res.*

- 106**, 7, 689-696 (2015).
- [7] P. Pietrusiewicz, M. Nabiałek, M. Dośpiał, K. Gruszka, K. Błoch, J. Gondro, P. Brągiel, M. Szota, Z. Stradomski, *J. All. Compd.* **615**, 1, 5 67-70 (2014).
- [8] S. Lesz, R. Babilas, M. Nabiałek, M. Szota, M. Dospiał, R. Nowosielski, *J. All. Compd.* 509 S197-S201 (2010).
- [9] K. Gruszka, M. Nabiałek, K. Błoch, J. Olszewski, *Nukleonika* **60**, No.1, (2015) 23-27.
- [10] M. G. Nabiałek, M. J. Dospiał, M. Szota, P. Pietrusiewicz, *J. Jedryka, J. All. Compd.* **509**, 3382-3386 (2011).
- [11] T. Holstein, H. Primakoff, *Phys. Rev.* **58**, 1098-1113 (1940).
- [12] K. Błoch, *J. Magn. Magn. Mater.* **390**, 118-122 (2015).
- [13] N. Lenge, H. Kronmüller, *Phys. Stat. Sol. (a)*, **95**, 621-633 (1986).
- [14] K. Błoch, M. Nabiałek, *Acta Phys. Pol. A* **127**, 442-444 (2015).
- [15] K. Błoch, M. Nabiałek, *Acta Phys. Pol. A* **127**, 413-414 (2015).
- [16] P. Gupta, A. Gupta, A. Shukla, Tapas Ganguli, A.K. Sinha, G. Principi, A. Maddalena, *J.App. Phys.*, 110 033537 (2011).